"Environmental Engineering" 10th International Conference
Vilnius Gediminas Technical University
Lithuania, 27–28 April 2017
http://enviro.vgtu.lt

eISSN 2029-7092 / eISBN 978-609-476-044-0

Article ID: enviro.2017.224
DOI: https://doi.org/10.3846/enviro.2017.224

High-rate GNSS Positioning for Precise Detection of Dynamic Displacements and Deformations: Methodology and Case Study Results

Jacek Paziewski[1], Rafal Sieradzki[2], Radoslaw Baryla[3]

[1,2,3] *Faculty of Geodesy, Geospatial and Civil Engineering, University of Warmia and Mazury in Olsztyn, Poland*
E-mails: [1]jacek.paziewski@uwm.edu.pl (corresponding author); [2]rafal.sieradzki@uwm.edu.pl; [3]baryla@uwm.edu.pl

Abstract. The monitoring of static and dynamic deformations of buildings and other engineering structures is of great interest for many scientific and practical reasons. Such measurements provide information required for safe maintenance of the constructions being a subject of various excitations. At present one of the most commonly used technology for this purpose is the high-rate GNSS positioning. The application of GNSS technology with appropriate processing methodology may meet the specific requirements which result in extraction of information on dynamic displacements and deformations of ground and engineering structures. The high temporal resolution and precision of GNSS phase observations predestine this technology to be applied to the most demanding applications in terms of accuracy, availability and reliability. In this study we present preliminary results of application of precise GNSS positioning for detection of small scale (centimeter level) dynamic displacements. In the first part of work there are described methodology and algorithms of precise coordinate estimation, involving both the relative positioning as well as the Precise Point Positioning technique. In the experiment both approaches were applied to monitor of antenna point variations on the basis of high-rate (20 Hz) observations processed in self-developed software. The dynamic displacements were simulated using specially constructed device moving GNSS antenna with dedicated amplitude and frequency. The obtained results indicate on possibility of detection of dynamic GNSS antenna displacements even at the level of millimetres using relative positioning. Moreover, the Precise Point Positioning approach has also proved its applicability to detect high-rate small scale changes of the controlled site coordinates.

Keywords: high-rate GNSS positioning, satellite geodesy, metrology, displacements, RTK, PPP.

Conference topic: Technologies of Geodesy and Cadastre.

Introduction

GNSS (Global Navigation Satellite Systems) is nowadays well-known and recognized technology contributing to a broad spectrum of applications such as navigation, geodesy, geodynamics, surveying etc. (Xu 2007; Popielarczyk, Templin 2013). In recent years this method has also been introduced to a number of new areas of science and engineering aimed at detection of various origin deformations and displacements (Malyszko *et al.* 2016). Such studies have mainly involved the analyses of ground movement caused by natural hazards and structural monitoring.

The potential of GNSS technology for detecting phenomena related to earthquakes was initially recognized and analysed by Larson (Larson *et al.* 2003). The further tests on this topic confirmed the applicability of satellite measurements to investigate of ground displacements being an effect of particular seismic events. In specific they make possible analysing waveform variations observed in estimated coordinates, offsets in GNSS permanent station positions and post seismic effects (Prawirodirdjo *et al.* 2010; Geng *et al.* 2016). In analogous way GNSS technology was adopted to investigate the displacements of surface observed during volcanic activity. Such analyses enabled the detection of deformations in the pre-eruptive phase as well as during the main phase of event (Mattia *et al.* 2008). As a consequence of high precision of GNSS results, the seismically active areas have been started to monitor using data from entire networks of permanent networks, i.e. GEONET (GPS Earth Observation Network System) or PBO (Plate Boundary Observatory). Taking into account a low-latency of such observations it is possible to detect seismic phenomena in near real time, what gives the opportunity to establish and maintain early warning systems (Blewitt *et al.* 2009).

Due to the development of receivers, GNSS technology has become also an important part of structural monitoring. Satellite measurements enable analyses of deformations observed for various structures such as bridges or tall buildings. Main purpose of such studies is predominantly behaviour of test object under different ambient excitations (Li *et al.* 2006; Yu *et al.* 2014). Their results, which are temporal variations of obtained coordinates, can support detailed description of the structure response on external conditions and allow the comparison of numerical models with real measurements (Kowalska *et al.* 2013). In contrast to research aimed at seismic displacements, where typi-

cally 1 s data are used, the analyses being a part of structural monitoring are performed with as high as possible time resolution (up to 100 Hz). As it was reported in previous research, the application of high-rate GNSS technology allow tracking the response of structures in frequency range from less than 0.2 Hz to even 10 Hz (Meng *et al.* 2007; Yi *et al.* 2013). Moreover, all these foregoing investigations confirmed that subcentimeter precision of GNSS-based coordinates makes possible the detection and evaluation of deformations being a result of different factors of impact such as wind or traffic.

The consequence of application of satellite measurements to deformation monitoring was also development of algorithms used within. Nowadays the detection of variations in estimated coordinates is generally realized using three approaches: relative positioning, precise point positioning (PPP) and phase residual method (PRM). The first one based on double differenced observations is the best recognized method of precise GNSS positioning (Xu 2007). Considering the relatively short baselines it ensures mitigation of common errors for both stations and as a result provides precise position in kinematic mode even in a single-epoch regime (Paziewski 2015). The second mentioned method is relied on undifferenced measurements (Kouba, Héroux 2001). Its precision is thus strictly related to the accuracy of implemented models, such as absolute phase center offsets and variations, and other input data (precise satellite orbits and clocks). PPP method is not considered as precise as relative positioning especially using short observational sessions. However, the previous studies confirmed that implementation of this approach in kinematic mode allows the detection of deformations as well. In contrast to both methods of positioning, the phase residual method does not provide direct information on coordinate changes but on changes of geometric distance between particular satellites and moving antenna. This purpose may be realized using time series of double differenced observations applying satellites at different elevations and azimuths (Schaal, Larocca 2002).

In this study there is presented an experiment aimed at detection of simulated small scale horizontal oscillations using 20 Hz GNSS observations. The variations of the antenna position were realized using specially designed device responsible for its periodic motion with different amplitudes. The main purpose of this work was detection of GNSS antenna position variations using relative and absolute methods of coordinate estimation and the comparison of results obtained for particular approaches in time and frequency domains. The results of GNSS analyses were performed with developed in-house software with implemented option of high-rate data processing. At this place it should be also mentioned that the processing of high-rate measurements in PPP mode is not supported by commercial software.

This contribution is organized as follows. In the next section the brief methodology for high-rate precise relative and precise point positioning is given. The following sections describe the experiment design and results of application of both approaches for detection of high-rate small scale oscillations. The last section is devoted to conclusions and disseminations.

Methodology

In order to extend the current knowledge on applicability of GNSS technology to deformation monitoring, this work presents the comparison of such results obtained using two methods of coordinate estimation: multi-GNSS precise relative and precise point positioning. Below we demonstrate a brief methodology for both approaches which were applied to simulated antenna displacements determination.

Precise relative positioning

In this study we adopt the geometry-based model for multi-GNSS relative positioning. The model is relied on the concept of double differencing of original carrier-phase and pseudorange signals and may be used in both static and kinematic modes. Many versions of the aforementioned approach have been developed so far. One of the most effective and well-recognized is so called ionosphere-weighted model which takes into account ionospheric delays parametrization (Bock *et al.* 2000; Odijk 2001; Paziewski 2016). As shown recent investigations this approach can be also modified in order to mitigate the influence of ionospheric disturbances (Sieradzki, Paziewski 2015). The ionosphere-weighted model is commonly applied for medium and long baselines reaching dozens of kilometres and more. Nevertheless in this study short (few kilometres long) and ultra-short (few metres long) baselines were used. Thus, the functional model could be simplified through neglecting the influence of the ionospheric delay. The integration of multi-constellation signals in a single relative positioning model requires a modification of the functional model and appropriate stochastic modelling of signals from independent GNSS constellations (Sieradzki, Paziewski 2016; Paziewski, Wielgosz 2017). For this study we adopted the loose combined approach. This was justified by using in processing different frequencies in both systems – L1 & L2 and E1 & E5a in the case of GPS and Galileo constellations respectively.

Below are given the simplified linearized equations of double differenced phase and pseudorange observables. The equations neglect the influence of the ionospheric delay. This generalized form of equations can be applied for any number of frequencies and constellations. In the case of loose integration Eq. (1) and (2) are formed separately for each of the applied constellation using independent pivot satellites.

$$\lambda_n \varphi^{ij}_{kl,\,n} = \rho^{ij}_{kl} + \lambda_n N^{ij}_{kl,\,n}; \tag{1}$$

$$P^{ij}_{kl,n} = \rho^{ij}_{kl}, \tag{2}$$

where: λ is the signal wavelength, φ is the carrier phase observable in cycles, P is the pseudorange, subscripts k, l and superscripts i, j denote stations and satellites respectively, ρ is the geometric range, N states for integer ambiguity, and finally n states for selected frequency.

The parameter estimation is performed using sequential least squares adjustment (Xu 2007). The vector of unknowns contains corrections to a priori values of stations coordinates and DD ambiguities. The zenith tropospheric delays are in this case treated as fixed values obtained from Modified Hopfield model and are mapped to slant delays using GMF mapping function (Goad, Goodman 1974; Boehm *et al.* 2006). The final solution is obtained after successful ambiguity resolution performed with the use of MLAMBDA method and validation with W-ratio test (Chang *et al.* 2005; Wang *et al.* 2009).

Precise Point Positioning

Recent rapid advances in the GNSS positioning algorithms led to development of the precise point positioning technique. Even if the concept itself is not new, nowadays we can recognize its several modifications. Ones of the research fields are these related to ambiguity resolution and multi-constellation signals application (Ge *et al.* 2008; Laurichesse *et al.* 2009; El-Mowafy *et al.* 2016). The determination of the absolute coordinates and its changes as well, predestines the PPP technique to displacements and deformation monitoring. In this case the position of the controlled site is related to global reference frames, which are realized by GNSS products such as satellites orbits and clocks. This led to possibility of abolishing the need of local reference sites establishment. As the PPP is based on absolute GNSS signals, the linearized observation equations of original undifferenced carrier-phase and pseudorange signals on selected frequency (n) can be expressed as follows:

$$\lambda_n \varphi^i_{k,n} = \rho^i_k + c\left(t_k - t^i\right) + \lambda_n \left(b_{k,n} - b^i_n\right) + \alpha^i_k ZTD_k - I^i_{k,n} + \lambda_n N^i_{k,n}; \tag{3}$$

$$P^i_{k,n} = \rho^i_k + c\left(t_k - t^i\right) + d_{k,n} + d^i_n + \alpha^i_k ZTD_k + I^i_{k,n}, \tag{4}$$

where: t_k is the receiver clock offset in seconds, t^i denotes the satellite clock correction in seconds, c is the speed of light in meters per second, b_k is the receiver uncalibrated phase delay in cycles, b^i denotes the satellite uncalibrated phase delay in cycles, d_k and d^i refer to the receiver and satellite code biases in meters, respectively, α is the troposphere mapping function coefficient, ZTD is the zenith tropospheric delay,

Well recognized approach in PPP is the utilization of double frequency observations and creation so called ionosphere-free (IF) linear combination (Kouba, Héroux 2001). The equations for carrier phase and code IF observables for each constellation can be written as:

$$\Phi^i_{k,IF} = \left(f_1^2 \Phi^i_{k,1} - f_2^2 \Phi^i_{k,2}\right) / \left(f_1^2 - f_2^2\right); \tag{5}$$

$$P^i_{k,IF} = \left(f_1^2 P^i_{k,1} - f_2^2 P^i_{k,2}\right) / \left(f_1^2 - f_2^2\right), \tag{6}$$

where: Φ is the phase observable in the units of meters on particular frequency (*IF*- ionosphere-free, *1*- first or *2*-second applied), f_1, f_1 are frequencies of two selected signals for each constellation (L1/L2 and E1/E5a in the case of GPS and Galileo satellites, respectively).

Since each satellite constellations has its own time scale we should take it into account e.g., in parametrization of the receiver clock parameters. One of the possibilities is the selection of the pivot reference time scale from applied GNSS systems and estimation of the between-system time difference parameter with respect to the former one. Alternatively, we can estimate individual receiver clock parameters for each constellation as it was done in our case. Finally, taking into account precise satellite orbits and clocks the observational model for each constellation on IF frequency can be denoted as below:

$$\Phi^i_{k,IF} = \rho^i_k + ct_k + B^i_{k,IF} + \alpha^i_k ZTD_k; \tag{7}$$

$$P^i_{k,IF} = \rho^i_k + ct_k + \alpha^i_k ZTD_k, \tag{8}$$

where: $B_{k,IF}$ denotes the phase ambiguity term on IF frequency combined with receiver and satellite initial phase biases and phase hardware delay biases.

The summary of the PPP and RTK processing strategies and models applied in this case study are given in Table 1.

Table 1. Details of PPP and RTK processing strategies

	PPP	**RTK**
Observables	Undifferenced ionosphere-free linear combination of phase and code GPS L1/L2 and Galileo E1/E5a	Double-differenced L1/L2 GPS and E1/E5a Galileo phase and code
Weighting	Elevation-dependent weighting	
Elevation angle cutoff	10°	
Sampling rate	0.05 s	
Troposphere delay modelling	A priori Modified Hopfield model + Global Mapping Function (GMF)	
Ionosphere delay modelling	First order of ionospheric delay eliminated by ionosphere-free linear combination	Elimination by double-differencing
Solution type	Kinematic float	Kinematic with ambiguity resolution
A priori standard deviation of observations	0.3 m and 0.002 m for raw code and phase of GPS and Galileo signals	
Satellite orbits and clocks	Precise from GFZ (orbits 15 min interval; clocks 30 s interval)	
Estimation method	Least squares with a priori parameter constraints	

Experiment design and results

The proposed experiment is aimed at practical performance assessment of described above both precise positioning approaches for determination of the high-rate dynamic horizontal displacements. The displacements of the GNSS antenna were intentionally simulated using specially designed device (Fig. 1). The GPS & Galileo signals were tracked using high-rate geodetic receivers: Javad Alpha + GrAnt G3T antenna (one as rover and one as close reference receiver), integrated with antenna Javad Triumph as second close reference station and Trimble NetR9 + TRM59800.00 SCIS antenna as third reference station located 4 km away from rover receiver. Thus, we had two ultra-short baselines connecting rover and reference stations (few meters long) and one short baseline (4 km long) which allowed establishment of several processing scenarios to be used in relative positioning. The rover antenna oscillated in East-West direction using two levels of amplitude: ~15 mm and ~34 mm, set for the first and second sessions respectively. The position of the rover antenna was determined in kinematic mode with sampling rate of 20 Hz using in-house developed scientific postprocessing software (Paziewski, Stepniak 2014; Paziewski 2015). Furthermore, several additional scenarios were designed in order to assess RTK positioning: GPS only solution vs. GPS+Galileo and double ultra-short baseline solution vs. single 4 km long baseline. Summary of all processing scenarios is given below:

1. RTK - single ultra-short baseline GPS+Galileo
2. RTK - double ultra-short baselines GPS
3. RTK - single 4 km baseline GPS
4. RTK - single 4 km baseline GPS+Galileo
5. PPP - GPS+Galileo

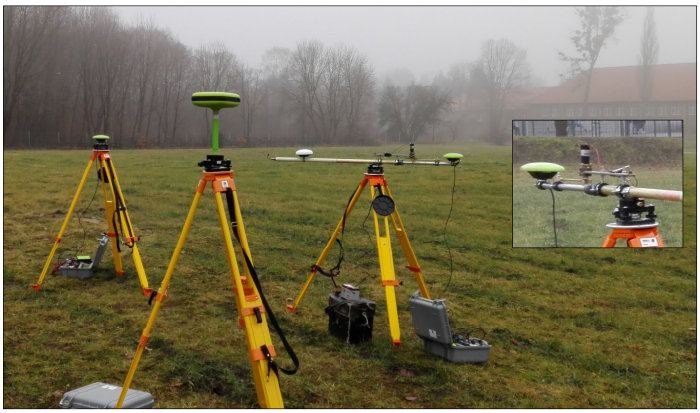

Fig. 1. GNSS equipment and device simulating antenna's displacements during field experiment

Since antenna displacements were simulated in E-W direction only these coordinate time series were analysed. The Figure 2 depicts example E-W coordinate time series derived from two examined approaches: high-rate kinematic PPP (scenario #5) – top panel and ultra-short double baseline RTK solution (scenario #2) – bottom panel. The initial part of the time series corresponds to period without any simulated displacements of the antenna, since during first ~6 minutes of the session rover receiver antenna was static.

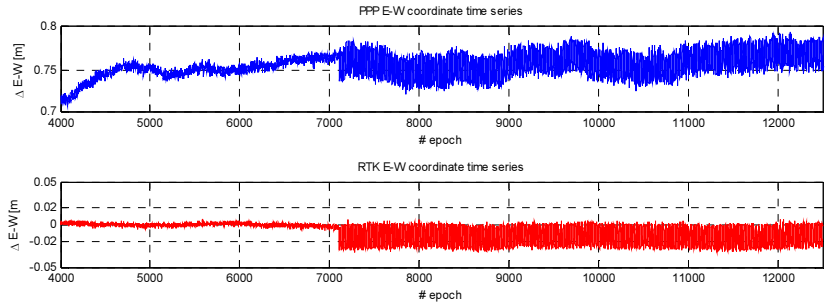

Fig. 2. PPP (top panel) and RTK (bottom panel) time series of rover receiver E-W coordinate variations during first session: static position of the antenna and simulated displacements

Preliminary examination of PPP results revealed their clear shift in respect to the reference coordinates of the rover antenna and slower variations, which are not associated with simulated movement. These effects are related to much longer convergence time required for precise point positioning, which typically affects the first minutes of session, as well as other not fully modelled factors (i.e. residual tropospheric delay). The first from the mentioned aspects is a result of a short observational session, which disenabled to obtain high accuracy of absolute position with PPP technique. Thus, it can be principally improved using longer time span of observations. The other factors are natural consequence of applied functional model and due to this fact their elimination during coordinate estimation is problematic. Despite these undesired effects one can also see clear short term changes of the E-W coordinates which reflect antenna's displacements simulated by device. Furthermore, in this regard there is a good coincidence between results obtained for both methods. In order to make possible the comparative analysis of displacements observed in PPP and RTK approaches, the offset and slower variations of results in PPP positioning were removed. For this goal it was used Butterworth filter of 6 order with cut-off period of 20s, what resulted in extraction of simulated oscillations. After this process the variations in coordinate time series can be considered only as relative displacements but they are still valuable for assumed analysis. The initial, static part of first session was also used to assess the noise of E-W coordinate time series of RTK and filtered values of PPP. The corresponding standard deviations reached the levels of 1.9 mm and 3.1 mm for relative and absolute solution respectively. These values can be treated as an indicator of expected precision of both methods.

The example variations of E-W component derived from RTK (scenario #2, bottom panels) and from filtered PPP (scenario #5, top panels) are given in Figures 3 (true amplitude of ~15 mm) and 4 (true amplitude of ~34 mm). In order to demonstrate the simulated displacements in a clear way, the figures intentionally cover only 2.5 minute part of all session. The differences in mean values of time series for both methods are caused by the filtration applied to the absolute positioning results. In this case zero value corresponds to average of coordinate time series. In the case of RTK, zero value refers to the initial position of GNSS rover antenna.

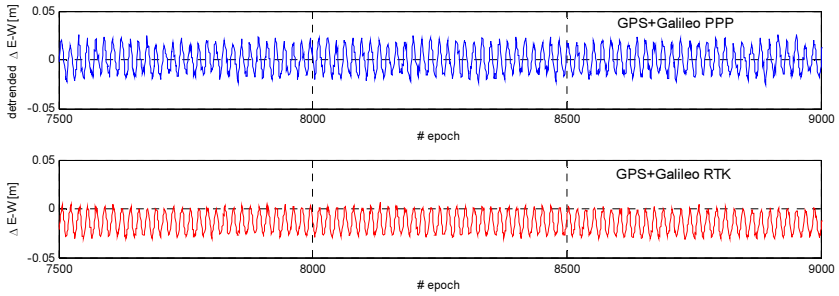

Fig. 3. Filtered PPP (strategy #5 top panel) and RTK (strategy #2 bottom panel) example time series of E-W coordinate during first session (true amplitude of 15.1 mm)

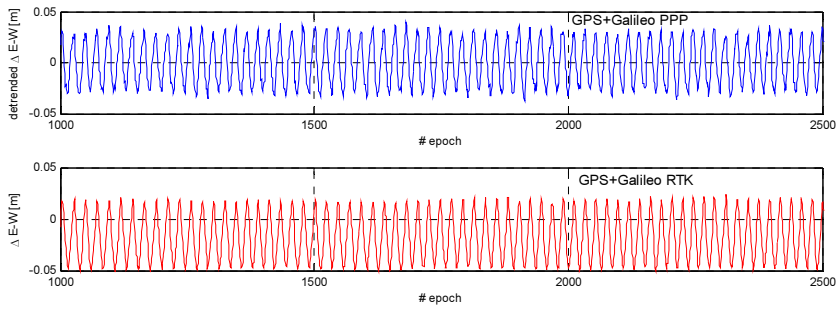

Fig. 4. Filtered PPP (strategy #5 top panel) and RTK (strategy #2 bottom panel) example time series of rover receiver E-W coordinate during second session (true amplitude of 33.9 mm)

The Figures 3 and 4 confirm that both relative and absolute positioning methods allow for identification of simulated displacements. The particularly precise and free from any low frequency components are results derived from the RTK method. It can be assumed that for such short sessions the accuracy of relative GNSS positioning is limited only by the noise of double differenced phase observations. In the case of filtered PPP time series, there are still observed the weak oscillations not associated with simulated displacements.

In order to provide more comprehensive view, the obtained results were investigated in frequency and time domains. The first analysis, aimed at evaluation of frequencies and amplitudes in obtained time series, was performed with Fourier transform. The examples of such results, presenting amplitude spectra computed for the same selected strategies (#2 and #5) and both session, are given in Figure 5. Basically, it confirms applicability of both methods to derive the information on analysed displacements. One can observe a full correspondence between dominant frequencies in raw RTK and filtered PPP time series, which equal 1.17 Hz and 0.86 Hz for the first and second session respectively. The change of simulated oscillations was unintended but it is not important for the purpose of our study. It was related to different resistance forces acting inside the device for both analysed amplitudes. Due to the mass of GNSS antenna it can be also expected that these forces are probably distinct for particular phases of movement, what in a consequence, caused the blurring of spectra in frequency domain.

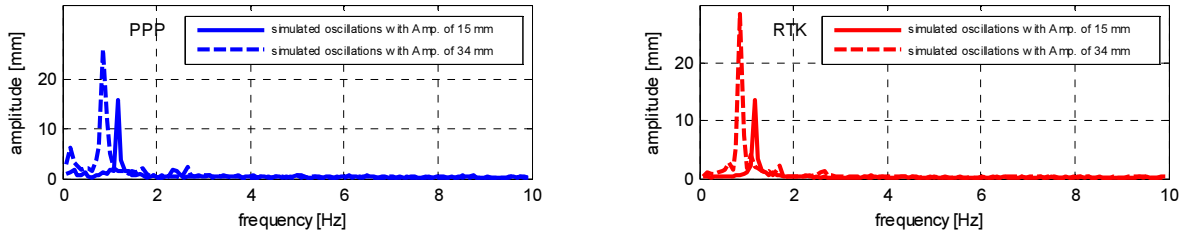

Fig. 5. Amplitude spectrum of the E-W coordinate changes obtained for relative ultra-short baselines positioning (scenario #2) – right panel and precise point positioning (scenario #5) – left panel

The results obtained for RTK scenario proved that estimated coordinates are practically free from any other frequency components. In the case of absolute positioning, FFT analysis confirmed the occurrence of residual effect of slower variations, which were characterized by ~6 mm amplitude for the second session. Comparing the amplitudes of displacement obtained for specific methods the results are also convergent at the level of ~2 mm (specific values are given in Tables 2 and 3).

In order to examine FFT-derived amplitudes, they are compared with the results obtained directly from time series and the true values of amplitudes. In the second case, the amplitudes were computed using averaging of maximal and minimal values observed for each cycle. Assuming that the noise is zero-mean, such values should be very precise. The true amplitude was precisely measured using calliper before the device installation. The summaries of empirically derived amplitudes for each scenario and both session are given in Tables 2 and 3. Considering the results obtained for different strategies of relative positioning one can see that values derived directly from time series are characterized by the error of ~0.2 mm. Only for the first strategy (single ultra-short baseline GPS+Galileo) the bias is higher and reached ~0.5 mm. It should be noted that lengthen of a baseline to ~4 km (scenarios #3 & #4) did not distort the results. Thus, such vectors can be also useful for structural monitoring with high precision. As it was expected, FT-derived amplitudes are underestimated for all relative scenario, what is related to blurring of dominant frequency. They differ from true values from 2 to 5 mm (13% of true amplitude).

Table 2. Empirical amplitude of the GNSS antenna displacements derived from FT and directly from time series (true amplitude = 15.1 mm)

Positioning strategy	FT derived amplitude [mm]	Average amplitude from time series [mm]
#1 Single ultra-short baseline GPS+Galileo	13.55	15.64
#2 Double ultra-short baselines GPS	13.64	15.26
#3 Single 4 km long baseline GPS	13.69	15.12
#4 Single 4 km long baseline GPS+Galileo	13.66	15.12
#5 PPP GPS+Galileo	15.83	19.03

Table 3. Empirical amplitude of the GNSS antenna displacements derived from FT and directly from time series (true amplitude = 33.9 mm)

Positioning strategy	FT derived amplitude [mm]	Average amplitude from time series [mm]
#1 Single ultra-short baseline GPS+Galileo	28.42	33.78
#2 Double ultra-short baselines GPS	28.40	33.62
#3 Single 4 km long baseline GPS	28.46	33.70
#4 Single 4 km long baseline GPS+Galileo	28.46	33.70
#5 PPP GPS+Galileo	26.16	32.68

More interesting are results obtained from PPP approach. It could be expected that the values from filtered PPP time series would be very precise as well. However, in the case of first session, the average amplitude is significantly overestimated and more importantly this effect cannot be related to the occurrence of residual low frequency component. It is thought that such result is related to accumulated solution of float ambiguity used in kinematic mode, which vary as a consequence of simulated displacements. This effect can be probably reduced through extending the initial part of session, what should allow stabilizing float ambiguity solution as well.

Conclusions

In this contribution we focus on assessing the applicability of the combined GPS+Galileo dual-frequency RTK positioning as well as based on ionosphere-free combination GPS+Galileo PPP for detection of high-rate dynamic horizontal displacements. The given results confirmed that both approaches can be an efficient tool in structural monitoring. In the case of relative positioning the precision of estimated horizontal components is at the level of phase noise of double differenced GNSS measurements. Furthermore, both ultra-short and short baselines are appropriate for such kind of analyses. Considering kinematic mode of PPP technique, the time series of coordinates may be affected by variations related to unmodelled factors and short convergence time. However, after their pre-processing it is also possible to achieve a millimeter level precision of horizontal displacements.

References

Blewitt, G.; Hammond, W. C.; Kreemer, C.; Plag, H.-P.; Stein, S.; Okal, E. 2009. GPS for real-time earthquake source determination and tsunami warning systems, *Journal of Geodesy* 83(3): 355–343. https://doi.org/10.1007/s00190-008-0262-5

Bock, Y.; Nikolaidis, R.; de Jonge, P. J.; Bevis, M. 2000. Instantaneous geodetic positioning at medium distances with the Global Positioning System, *Journal of Geophysical Research* 105(B12): 28233–28253. https://doi.org/10.1029/2000JB900268

Boehm, J.; Niell, A.; Tregoning, P. *et al.* 2006. Global Mapping Function (GMF): A new empirical mapping function based on numerical weather model data, *Geophysical Research Letters* 33: L07304. https://doi.org/10.1029/2005GL025546

Chang, X. W.; Yang, X.; Zhou, T. 2005. MLAMBDA: a modified LAMBDA method for integer least-squares estimation, *Journal of Geodesy* 79: 552–565. https://doi.org/10.1007/s00190-005-0004-x

El-Mowafy, A.; Deo, M.; Rizos, C. 2016. On biases in Precise Point Positioning with multi-constellation and multi-frequency GNSS data, *Measurement Science and Technology* 27(3): 035102. https://doi.org/10.1088/0957-0233/27/3/035102

Ge, M.; Gendt, G.; Rothacher, M.; Shi, C.; Liu, J. 2008. Resolution of GPS carrier phase ambiguities in Precise Point Positioning (PPP) with daily observations, *Journal of Geodesy* 82: 389–399. https://doi.org/10.1007/s00190-007-0187-4

Geng, T.; Xie, X.; Fang, R.; Su, X.; Zhao, Q.; Liu, G.; Li, H.; Shi, C.; Liu, J. 2016. Real-time capture of seismic waves using high-rate multi-GNSS observations: Application to the 2015 Mw 7.8 Nepal earthquake, *Geophysical Research Letters* 43: 161–167. https://doi.org/10.1002/2015GL067044

Goad, C. C.; Goodman, L. 1974. A modified Hopfield tropospheric refraction correction model, in *American Geophysical Union Annual Fall Meeting*, 12–17 December 1974, San Francisco, California, USA.

Kouba, J.; Héroux, P. 2001. Precise point positioning using IGS orbit and clock products, *GPS Solutions* 5(2): 12–28. https://doi.org/10.1007/PL00012883

Kowalska, E.; Rutkiewicz, A.; Małyszko, L. 2013. Static and dynamic characteristic of masonry bridge using laser scanning and finite elements, in J. Obrębski, L. Małyszko (Eds.). L*ightweight Structures in Civil Engineering – LSCE 2013 Contemporary Problems*. Warszawa-Olsztyn, 70–76.

Larson, K. M.; Bodin, P.; Gomberg, J. 2003. Using 1-Hz GPS data to measure deformations caused by the Denali fault earthquake, *Science* 300: 1421–1424. https://doi.org/10.1126/science.1084531

Laurichesse, D.; Mercier, F.; Berthias, J. P.; Brocca, P.; Cerri, L. 2009. Integer ambiguity resolution on undifferenced GPS phase measurements and its application to PPP and satellite precise orbit determination, *Navigation* 56(2): 135–149. https://doi.org/10.1002/j.2161-4296.2009.tb01750.x

Li, X.; Ge, L.; Ambikairajah, E.; Rizos, C.; Tamura, Y.; Yoshida, A. 2006. Full-scale structural monitoring using an integrated GPS and accelerometer system, *GPS Solutions* 10: 233–247. https://doi.org/10.1007/s10291-006-0023-y

Malyszko, L.; Kowalska, E.; Paziewski, J.; Rutkiewicz, A.; Sieradzki, R. 2016. Monitoring of structural vibration using GNSS and accelerometer data – preliminary tests, Chapter 6 in L. Małyszko, R Tarczewski (Eds.). *Lightweight Structures in Civil Engineering – LSCE 2016 Contemporary Problems*. Olsztyn, 37–42.

Mattia, M.; Palano, M.; Aloisi, M.; Bruno, V.; Bock, Y. 2008. High rate GPS data on active volcanoes: an application to the 2005–2006 Mt. Augustine (Alaska, USA) eruption, *Terra Nova* 20(2): 134–140. https://doi.org/10.1111/j.1365-3121.2008.00798.x

Meng, X.; Dodson, A. H.; Roberts, G. W. 2007. Detecting bridge dynamics with GPS and triaxial accelerometers, *Engineering Structures* 29: 3178–3184. https://doi.org/10.1016/j.engstruct.2007.03.012

Odijk, D. 2001. Instantaneous precise GPS positioning under geomagnetic storm conditions, *GPS Solutions* 5(2): 29–42. https://doi.org/10.1007/PL00012884

Paziewski, J. 2015. Precise GNSS single epoch positioning with multiple receiver configuration for medium-length baselines: methodology and performance analysis, *Measurement Science and Technology* 26(3): 035002. https://doi.org/10.1088/0957-0233/26/3/035002

Paziewski, J. 2016. Study on desirable ionospheric corrections accuracy for network-RTK positioning and its impact on time-to-fix and probability of successful single-epoch ambiguity resolution, *Advances in Space Research* 57(4): 1098–1111. https://doi.org/10.1016/j.asr.2015.12.024

Paziewski, J.; Stepniak, K. 2014. New on-line system for automatic postprocessing of fast-static and kinematic GNSS data, in D. Cygas, T. Tollazzi (Eds.). *9th International Conference on Environmental Engineering – selected papers*, 22–23 May 2014, Vilnius, Lithuania.

Paziewski, J.; Wielgosz, P. 2017. Investigation of some selected strategies for multi-GNSS instantaneous RTK positioning, *Advances in Space Research* 59(1): 12–23. https://doi.org/10.1016/j.asr.2016.08.034

Popielarczyk, D.; Templin, T. 2013. Application of integrated GNSS/hydroacoustic measurements and GIS geodatabase models for bottom analysis of Lake Hancza: the deepest inland reservoir in Poland, *Pure and Applied Geophysics* 171(6): 997–1011. https://doi.org/10.1007/s00024-013-0683-9

Prawirodirdjo, L.; McCaffrey, R.; Chadwell, C. D.; Bock, Y.; Subarya, C. 2010. Geodetic observations of an earthquake cycle at the Sumatra subduction zone: Role of interseismic strain segmentation, *Journal of Geophysical Research* 115: B03414. https://doi.org/10.1029/2008JB006139

Schaal, R. E.; Larocca, A. P. C. 2002. A methodology for monitoring vertical dynamic sub-centimeter displacements with GPS, *GPS Solutions* 5(3): 15–18. https://doi.org/10.1007/PL00012895

Sieradzki, R.; Paziewski, J. 2015. MSTIDs impact on GNSS observations and its mitigation in rapid static positioning at medium baselines, *Annals of Geophysics* 58(6): A0661.

Sieradzki, R.; Paziewski, J. 2016. Comparative assessment of multi-GNSS phase measurements noise, in *IAG Commission 4 Symposium*, 4–7 September 2016, Wroclaw, Poland.

Wang, B.; Miao, L.; Wang, S.; Shen, J. 2009. A constrained LAMBDA method for GPS attitude determination, *GPS Solutions* 13(2): 97–107. https://doi.org/10.1007/s10291-008-0103-2

Xu, G. 2007. GPS: *theory, algorithms and applications*. 2nd ed. Berlin Heidelberg Springer-Verlag.

Yi, T. H.; Li, H. N.; Gu, M. 2013. Experimental assessment of high-rate GPS receivers for deformation monitoring of bridge, *Measurement* 46: 420–432. https://doi.org/10.1016/j.measurement.2012.07.018

Yu, J.; Meng, X.; Shao, X.; Yan, B.; Yang, L. 2014. Identification of dynamic displacements and modal frequencies of a medium-span suspension bridge using multimode GNSS processing, *Engineering Structures* 81: 432–443. https://doi.org/10.1016/j.engstruct.2014.10.010